International Journal of Modern Physics E
Vol. 30, No. 8 (2021) 2150072 (13 pages)

DOI: 10.1142/S0218301321500725

World Scientific
www.worldscientific.com

Particle ratios within EPOS, UrQMD and thermal models at AGS, SPS and RHIC energies

Mahmoud Hanafy*

Faculty of Science, Physics Department,
Benha University 13518, Benha, Egypt
and
World Laboratory for Cosmology and Particle Physics (WLCAPP),
11571 Cairo, Egypt

Abdel Nasser Tawfik

Egyptian Center for Theoretical Physics (ECTP),
Nile University,
Juhayna Square off 26th-July-Corridor 12588 Giza, Egypt
and
Institute for Theoretical Physics, Goethe University,
Max-von-Laue-Str. 1, D-60438 Frankfurt am Main, Germany

Muhammad Maher

Faculty of Science, Physics Department,
Helwan University, Ain Helwan,
P. O. 11795, 11795 Cairo, Egypt
and
World Laboratory for Cosmology and Particle Physics (WLCAPP),
11571 Cairo, Egypt
m.maher@science.helwan.edu.eg

Werner Scheinast

Joint Institute for Nuclear Research,
Veksler and Baldin Laboratory of High Energy Physics,
Moscow Region 141980 Dubna, Russia

Received 5 May 2021
Revised 22 July 2021
Accepted 6 August 2021
Published 16 September 2021

The particle ratios k^+/π^+, π^-/K^-, $\bar{p}/\pi^-$, Λ/π^-, Ω/π^-, p/π^+, π^-/π^+, K^-/K^+, $\bar{p}/p$, $\bar{\Lambda}/\Lambda$, $\bar{\Sigma}/\Sigma$, $\bar{\Omega}/\Omega$ measured at AGS, SPS and RHIC energies are compared with large statistical ensembles of 100,000 events deduced from the CRMC EPOS 1.99 and the Ultra-relativistic Quantum Molecular Dynamics (UrQMD) hybrid model. In the UrQMD hybrid model two types of phase transitions are taken into account. All these data are

*Corresponding author.

then confronted with the ideal Hadron Resonance Gas Model. The two types of phase transitions are apparently indistinguishable. Apart from k^+/π^+, k^-/π^-, Ω/π^-, $\bar{p}/\pi^+$ and $\bar{\Omega}/\Omega$, the UrQMD hybrid model agrees well with the CRMC EPOS 1.99. We also conclude that the CRMC EPOS 1.99 seems to largely underestimate k^+/π^+, k^-/π^-, Ω/π^- and $\bar{p}/\pi^+$.

Keywords: Hadron resonance gas; UrQMD; particles ratios; CRMC; EPOS 1.99.

PACS Number(s): 24.60.−k, 25.75.−q, 02.50.Ng

1. Introduction

In nuclear collisions, the statistical nature of the particle production allows the utilization of the particle ratios, for instance, to conduct systematic studies on the thermal properties of the final state. Over the last few decades, huge experimental data at energies covering up four orders of magnitude of GeV are now available. It turns out that various statistical thermal models[1–8] are remarkably successful in explaining the resulting particle yields and their ratios measured in heavy-ion collisions. Such a huge data set allowed us to draw the conclusion that the produced particles seem reaffirming the assumption that the hadrons are likely stemming from thermal sources with given temperatures and given chemical potentials. It becomes obvious that such a thermal nature is valid, universally, except for a few baryon-to-meson ratios, such as proton-to-pion at top RHIC and LHC, known as proton anomaly.[9]

Besides the statistical nature of the particle production, another main goal of the nuclear collisions is the detection of unambitious signatures for the possible hadron-quark phase transition.[10] This can, among others, allow us to verify the theory of strong interaction, the quantum chromodynamics (QCD), which predicts that the hadronic matter likely undergoes phase transition(s) from confined colorless hadrons to deconfined colored quark-gluon plasma (QGP) or vice versa.[1] So far various nuclear experiments gave indirect signatures for the existence of the QGP phase, for example, Refs. 11 and 12. So far, we understand that the order of the phase transition, especially at low baryon chemical potential, is a rapid crossover.[9,13,14]

It was argued that at equilibrium the particle ratios are well explained by two variables; the freezeout temperature ($T_{\mathtt{ch}}$) and the baryon chemical potential ($\mu_{\mathtt{b}}$). In nuclear collisions, the freezeout stage occurs where the inellastic reactions cease and the number of produced particles becomes fixed. At this stage, the thermal models, such as the hadron resonance gas (HRG) model, determine essential characteristics for dense and hot fireball generated in the heavy-ion collisions. As a result, the thermal models are utilized as an essential tool connecting the QCD phase diagram with the nuclear experiments,[15,16] in the sense that the measurements, mainly the particle multiplicities, are connected to the number density in the thermal models, which in turn are strongly dependent on chemical freezeout parameters; $T_{\mathtt{ch}}$ and $\mu_{\mathtt{b}}$. In this way, we speak of thermodynamics, correlations, fluctuations, etc. in nuclear collisions.[2]

The dependence of $\mu_{\mathtt{b}}$ and $T_{\mathtt{ch}}$ on the nucleon–nulceon center-of-mass energies $\sqrt{s_{\mathtt{NN}}}$ constructs a boundary of the chemical freezeout diagram which is very close to the QCD phase diagram.[17] The dependence of $T_{\mathtt{ch}}$ on $\mu_{\mathtt{b}}$ looks similar to that of the various thermodynamic quantities as calculated in the lattice QCD,[15,16] which in turn are reliable quantities, especially at $\mu_b/T \leq 1$, i.e., at $\sqrt{s_{\mathtt{NN}}}$ greater than that of top SPS energies. Accordingly, these boundaries remain featured,[18] at lower energies, i.e., larger baryon chemical potential, where the QCD-like effective models, such as the HRG model[2] and the Polyakov linear-sigma model (PLSM)[9,14] play a major role. The hybrid event-generators such as the Cosmic Ray Monte Carlo (CRMC)[19–28] models and the Ultra-relativistic Quantum Molecular Dynamic (UrQMD) v3.4[29–34] are the frameworks, which we are going to compare with the available experimental results and with calculations based on the thermal models, as well.

This work presents predictions for the future facilities such as the Nuclotron-based Ion Collider fAcility (NICA) future facility at the Joint Institute for Nuclear Research (JINR), Dubna-Russia and the Facility for Antiproton and Ion Research (FAIR) at the Gesellschaft für Schwerionenforschung (GSI), Darmstadt-Germany. These and the BES-II program at RHIC are designed to cover the intermediate temperature region of the QCD phase diagram, while both LHC and top RHIC obviously operate at low $\mu_{\mathtt{b}}$ or high $T_{\mathtt{ch}}$, i.e., left part of the QCD phase-diagram.

In this paper, we compare various particle ratios deduced from CRMC and UrQMD v3.4 with the HRG calculations.[18] The latter would allow us to adjust $T_{\mathtt{ch}}$ and $\mu_{\mathtt{b}}$, if we primarily were interested in statistical fits. In this study, we aren't targeting any statistical fits. We concretely aim at comparing these three sets of results, namely the experimental results, the results deduced from the two event generators, and the HRG calculations. The latter use a combination of $T_{\mathtt{ch}}$ and $\mu_{\mathtt{b}}$ in order to deduce various particle yields and ratios, at a wide range of energies. Here, we focus on energies ranging from 7.7 to $\sim$200 GeV. In the HRG calculations, both $T_{\mathtt{ch}}$ and $\mu_{\mathtt{b}}$ are conditioned to one of the universal freezeout conditions,[18] such as constant entropy density normalized to $T^3_{\mathtt{ch}}$,[35,36] constant higher moments of the particle multiplicity,[37,38] constant trace anomaly[39] or an analogy of the Hawking-Unruh radiation.[40]

With this reference, we highlight that two types of the phase transitions are taken into account in UrQMD, namely, first order and crossover. We emphasize that the HRG model, which is a good statistical approach of various thermodynamic quantities, such as the particle density, can't be utilized for phenomena like deconfinement and chiral phase transition(s).[18] However, HRG describes well the hadron phase.[2] Different stages of the colliding systems covering from early stages up to the final state of the particle production can be characterized in UrQMD v3.4[41] and in CRMC.[19] Out of the various types of the nucleus–nucleus collisions in CRMC, we utilize the hadronic interacting model namely EPOS 1.99. Having all these prepared, a direct comparison with the experimental results can be achieved.

This paper is organized as follows. Section 2 gives short reviews on the different approaches; HRG, UrQMD v3.4 and CRMC EPOS 1.99. In Sec. 3, the results on different particle ratios are presented. Section 4 is devoted to the final conclusions.

2. Approaches and Event Generators

In this section, we give a short description on the Cosmic Ray Monte Carlo Code (CRMC EPOS 1.99) and the Ultrarelativistic Quantum Molecular Dynamic (UrQMD) hybrid approaches which shall be used in calculating various particle ratios at energies spanning between $\sqrt{s_{\rm NN}} = 7.7$ and 200 GeV. The comparison between the results from CRMC and UrQMD v3.4 event generators and that from the HRG model with AGS, SPS and RHIC experiment is novel on one-hand side. On the other hand, this allows us to conduct a systematic study. We aim at understanding whether both even generators CRMC and UrQMD v3.4 are able to give particle ratios compatible to the experiments and accordingly shed light on dynamics of the particle production and how this would be depending on the beam energy. Furthermore, this would help in validating both event generators in estimating different particle ratios and simultaneously deducing the freezeout parameters, especially at energies where experimental results aren't available so far and/or where FAIR and NICA shall be operating.

2.1. *Hadron resonance gas model*

As per Hagedorn, the formation of resonances is to be understood in a bootstrap picture, i.e., the resonances or fireballs are conjectured to be composed of further resonances or fireballs, which in turn are consistent of lighter resonances or smaller fireballs and so on. The thermodynamic properties of such a system can be derived directly from the partition function $Z(T, \mu, V)$. In a grand canonical ensemble, this reads[2]

$$Z(T, V, \mu) = \mathrm{Tr}\left[\exp\left(\frac{\mu N - H}{T}\right)\right], \tag{1}$$

where H is Hamiltonian combining all relevant degrees of freedom (dof) in deconfined and strongly interacting system and N is the number of constituents, e.g., dof. In the HRG model, Eq. (1) can be expressed as a sum over all hadron resonances.[2] The hadron data used in the present calculations are taken from the recent particle data group[42]

$$\ln Z(T, V, \mu) = \sum_i \ln Z_i(T, V, \mu) = \frac{V g_i}{2\pi^2} \int_0^\infty \pm p^2 dp \ln\left[1 \pm \lambda_i \exp\left(\frac{-\varepsilon_i(p)}{T}\right)\right], \tag{2}$$

where $\pm$ stands for bosons and fermions, respectively, $\varepsilon_i = (p^2 + m_i^2)^{1/2}$ is the dispersion relation of the ith particle and λ_i is its fugacity factor[2]

$$\lambda_i(T, \mu) = \exp\left(\frac{B_i \mu_{\rm b} + S_i \mu_S}{T}\right), \tag{3}$$

where $B_i(\mu_{\mathtt{b}})$ and $S_i(\mu_S)$ are baryon and strange quantum numbers (their corresponding chemical potentials) of the ith hadron, respectively.

The number density can be deduced as

$$n_i(T,\mu) = \sum_i \frac{\partial \ln Z_i(T,V,\mu)}{\partial \mu_i} = \sum_i \frac{g_i}{2\pi^2} \int_0^\infty \frac{p^2 dp}{\exp\left[\dfrac{\mu_i - \varepsilon_i(p)}{T}\right] \pm 1}. \tag{4}$$

The temperature T and the chemical potential $\mu = B_i\mu_{\mathtt{b}} + S_i\mu_S + \cdots$ are related to each other and in turn each of them is related to $\sqrt{s_{\mathtt{NN}}}$.[2] As an overall equilibrium is assumed, μ_S is taken as a dependent variable to be estimated due to the strangeness conservation, i.e., at given T and $\mu_{\mathtt{b}}$, a value assigned to μ_S has to assure that $\langle n_S\rangle - \langle n_{\bar{S}}\rangle$ vanishes. Only then, μ_S joins T and $\mu_{\mathtt{b}}$ in determining further thermodynamic calculations, such as the particle yields and the ratios. Chemical potentials for other quantum charges, such as electric change and isospin, can also be determined as functions of T, $\mu_{\mathtt{b}}$ and μ_S and each must fulfill the corresponding laws of conversation.

The key mechanism at this stage of the final expansion is unstable resonance decay. As a result, the ultimate number density for ith particle is given as

$$n_i^{\text{final}} = n_i + \sum_j Br_{j\to i} n_j, \tag{5}$$

where $Br_{j\to i}$ is the effective branching ratio of jth hadron resonance into ith particle. Taking into consideration all multi-step decay cascades, then

$$Br_{j\to i} = br_{j\to i} + \sum_{i_1} br_{j\to i_1} br_{i_1\to i} + \sum_{i_1,i_2} br_{j\to i_1} br_{i_1\to i_2} br_{i_2} + \cdots, \tag{6}$$

where $br_{j\to i}$ is the branching ratio jth hadron resonance into ith hadron. In this paper, we incorporate contributions from hadrons (55 different baryon species and 32 different mesons species) and their resonances composed of light and heavy flavored particles with mass up to 11 GeV as well as their antiparticles identified in the Particle Data Group.[43] Reference 43 is also used for the decay branching ratios.

We employ the complete grand-canonical statistical set of the thermodynamic parameters in our calculations for ideal hadron gas model with pointlike hadrons. Corrections resulting from van der Waals repulsive interactions and excluded volume corrections have not been considered. Although we do not employ the Boltzmann approximation, we can assume it for the sake of simplicity in order to show which parameters the particle ratios are dependent on. The particle ratios are calculated using Eq. (5), where the baryon chemical potential and the temperature are replaced in terms of the center of mass energy $\sqrt{S_{\mathrm{NN}}}$[44]

$$\mu_B = \frac{a}{1 + b\sqrt{S_{\mathrm{NN}}}}, \tag{7}$$

where $a = 1.245 \pm 0.094\,\mathrm{GeV}$ and $b = 0.264 \pm 0.028\,\mathrm{GeV}^{-1}$. The temperature can also be defined in terms of the center-of-mass energy.[44]

$$T = T_{\mathrm{lim}}\left[\frac{1}{1+\exp\left(\frac{1.172-\log(\sqrt{S_{\mathrm{NN}}})}{0.45}\right)}\right], \tag{8}$$

where $\sqrt{S_{\mathrm{NN}}}$ is taken in GeV, and $T_{\mathrm{lim}} = 161 \pm 4\,\mathrm{MeV}$.

2.2. *Ultrarelativistic quantum molecular dynamic model*

The UrQMD hybrid model[29–34,45] assumes a nonhomogeneous medium and combines various advantages of the hadronic transport theory and ideal fluid dynamics, as well. From the hydrodynamic evolution, the UrQMD hybrid model is conjectured to simulate almost the entire evolution of the heavy-ion collisions starting from a very early stage up to the final state of the particle production. Because of the different dynamics, symmetries and effective dof, for instance, the different stages are apparently distinguishable from each other. Therefore, different theoretical approaches must be utilized. On the other hand, the hydrodynamic models, which excellently describe the various stages of the nuclear collisions integrated in the UrQMD hybrid models furnish this with a unified framework, which in turn manifest the characteristics of the different stages. Furthermore, the large interaction rate and the microscopic Boltzmann transport models are also embedded. All these provide the UrQMD hybrid models with tools for a good description of the matter at low interaction rates.

For a hybrid event, we begin with UrQMD in cascade mode. Then, the nuclei are initialized and brought to collision. The hydrodynamic evolution starts when the nuclei with given radii r have passed through each other. The corresponding temporal expansion $t_{\mathrm{hadro}} = 2r(\gamma^2-1)^{1/2}$, where γ is the Lorentz factor. Assuming a local thermal equilibrium in each hydro cell, the so far produced particles are mapped onto a hydrodynamic grid. When the energy density of all hydro cells in a transverse slice with thickness 0.2 fm drops to 20% of the nuclear ground state density, the hydro dof in this slice are finally mapped to particles (Cooper–Frye equation).

The UrQMD hybrid model is a realistic and a well-tested model for the background medium. It is a widely utilized event generator based on a large number of solutions of the Monte Carlo technique for a great number of partial differential equations giving the evolution of the phase-space densities and has a great number of unknown parameters which could be fixed from theoretical postulates and experimental results. Ingredients such as event-by-event fluctuations are included so that in this environment even the heavy quarks (charm and bottom) are placed in the nucleus–nucleus collision space-time-coordinates and allowed to propagate at each hydro time step in the hot medium by using the correspondent cell properties such

as velocities, temperatures and length of time-step (Langevin approach). At each time step and temperature, all particles are checked regarding being hadronized.

In this work, we implement the UrQMD hybrid event generator version 3.4[29] at various beam energies 7, 7.7, 9, 11, 11.5, 13, 19, 19.6, 27, 39, 62.4, 130 and 200 GeV in standard parameter calculations. The fact that two different types of phase transition, namely, crossover and first order, are possible, allows us to run the UrQMD simulations for each of them, separately. This enables the characterization of the possible studies of the hadronization processes on the last-state particle production. With this we wanted to investigate which type of the phase transition matches well with the experimental results. To illustrate this point, we recall that the measurements, which are multiplicities of produced particles either in 4π detector acceptance and/or with limited rapidity, transverse momentum, etc. aren't providing any direct signature on the order of the phase transition. The latter was obtained in the first-principle lattice QCD and QCD-like approaches.

In hybrid UrQMD version 3.4, The equation of state (EoS) for fluid dynamical evolution in the case of crossover is drawn from the SU(3) parity doublet model, which includes quark dof in addition to the thermal contribution of the Polyakov loop.[46,47] This EoS agrees qualitatively with lattice QCD results at vanishing baryon chemical potentials and, more critically, is conjectured to be applicable at finite baryon chemical potentials as well. An EoS from the SU(2) bag model must be incorporated for first-order phase transition. The active EoS is converted to the one that characterises the hadron gas by the end of the hydrodynamical evolution. As a result, the active dof on both sides of the transition hypersurface are guaranteed to be identical.[46,47] In UrQMD v. 3.4, the technique proposed in Ref. 48 is used for the first-order phase transition. The hadron matter phase is characterized by the a — type model, while the quark-gluon plasma is described by the MIT bag model, with a first-order phase transition between the two phases.

We underline two differences between crossover and first-order phase transitions[34] for completeness' sake: latent heat and dof. Both are greater in first-order phase transition than in crossover. Furthermore, the transition from pure hadron to parton matter occurs gradually, implying that a rather large range of temperatures is required to convert the QCD matter from pure hadron to parton matter.[41] There is some influence of a technological feature of UrQMD on its physical outcome as a constraint. There may be some bias in the generated particle statistics when the software transitions from the hydrodynamical treatment of the high-density stage of the hadronic medium back to the "regular" particle-based transport code.[34] The differences in particle ratios between first order and crossover phases may appear lower than predicted by the physical model since we used the same particlization process in both situations.

From an ensemble of at least 100,000 events generated by the UrQMD hybrid model, we have calculated the ratios of different particle yields, at different center-of-mass energies 7, 7.7, 9, 11, 11.5, 13, 19, 19.6, 27, 39, 62.4, 130 and 200 GeV.

In doing this, two types of phase transitions are taken into consideration: first order and crossover. The results are compared with the ones calculated from the HRG model and generated by CRMC EPOS 1.99, are confronted to the available experimental results.

2.3. *Cosmic ray Monte carlo (CRMC) model*

EPOS is a parton model with many binary parton–parton interactions creating parton ladders. EPOS integrates energy-sharing for cross-section calculations, particle production, parton multiple scattering, outshell remnants, screening and shadowing via unitarization and splitting, and collective effects for dense media. Concretely, CRMC is a project incorporating an interface to the cosmic rays models for effective QCD-like models, Pierre Auger Observatory and high-energy experiments such as NA61, LHCb, TOTEM, ATLAS and CMS experiments. The cosmic ray models are built on top of the Gribov–Regge model such as EPOS 1.99/LHC. CRMC offers a complementary description for the background including diffraction and also provides a common interface to access the output from various event generators for nuclear collisions. The interface is linked to a wide range of models, however, the unique focus is to models using simulations of extensive cosmic ray air showers such as qgsjet01,[19,20] qgsjetII,[21–23] sibyII,[24–26] EPOS 1.99,[27,28] QGSJET01 and SIBYII2.3, at low energies. At high energies, EPOS 1.99/LHC and QGSJETII v03 and v04 are the ones to be integrated together.

EPOS is designed for the cosmic ray air showers and can be applied to pp- and AA-collisions at SPS, RHIC and LHC energies. EPOS utilizes a simplified treatment of the interactions in the final state and can be used for minimum bias hadronic interactions in heavy-ion interactions.[49] It is worthy emphasizing that EPOS — even in the final state — doesn't cover the simulations for full hydro system. EPOS 1.99/LHC is a model utilized in the present calculations, has a large number of parameters describing the essential quantities in physics and the phenomenological postulates. These can be fixed through experimental and theoretical assumptions. It is assumed that EPOS 1.99/LHC draws a reasonable picture about the interactions between hadrons regarding the data generated from available experiments and event generators.

In this work, we use EPOS 1.99 event generator at different center-of-mass energies 7, 7.7, 9, 11, 11.5, 13, 19, 19.6, 27, 39, 62.4, 130 and 200 GeV in standard parameter calculations. We have generated ensembles of at least 100,000 events (at each of these energies). Proving the validity of EPOS 1.99, we aim at predicting the corresponding particle ratios estimated at the freezeout parameters, which are novel predictions for the future facilities FAIR and NICA.

3. Results and Discussion

The present analysis is focused on characterizing results measured at STAR BES-I energies[50] and partially at the Alternating Gradient Synchrotron (AGS)[3]

Table 1. The dependence of the freeze-out parameters on the center-of-mass energy.

$\sqrt{S_{\rm NN}}$GeV	μ GeV	T GeV
7	0.733 ± 0.005	0.052 ± 0.006
7.7	0.718 ± 0.007	0.056 ± 0.005
9	0.694 ± 0.006	0.061 ± 0.006
11	0.663 ± 0.007	0.069 ± 0.007
11.5	0.656 ± 0.0065	0.070 ± 0.007
13	0.638 ± 0.007	0.075 ± 0.006
19	0.578 ± 0.005	0.090 ± 0.009
19.6	0.574 ± 0.007	0.091 ± 0.005
27	0.520 ± 0.0052	0.103 ± 0.001
39	0.470 ± 0.004	0.115 ± 0.0011
62.4	0.404 ± 0.004	0.128 ± 0.005
130	0.310 ± 0.003	0.143 ± 0.005
200	0.263 ± 0.003	0.149 ± 0.008

and the Superproton Synchrotron (SPS)[1] energies, as well, such as NA49,[51–53] NA44[51–55] and NA57.[56] A great part of this range of the beam energy shall be accessed by NICA and FAIR future facilities.[57] In the figures, the calculations from CRMC EPOS 1.99 (stars),[27,28] and from UrQMD hybrid model[30–34] with first-order (crosses) and crossover phase-transition (empty circles), where the rapidity Y and transverse momentum P_t are taken according to the STAR detector ($1.1 < Y(\mathrm{GeV/C}) < 2.6$ and $0.005 < P_t(\mathrm{GeV/C}) < 5$), are compared with the HRG calculations (solid curves),[1–8] as well. The dependence of the freeze-out parameters on the center-of-mass energy is shown in Table 1.

Figure 1 shows the energy dependence of the particle ratios (a) k^+/π^+,[52,53,56] (b) π^-/K^-,[52,53,56,58] (c) $\bar{p}/\pi^-$,[52,53,56,59] (d) Λ/π^-,[52–54,56,58,60–62] (e) Ω/π^-[52–54,56,58,60–62] and (f) p/π^+[52–54,56,58,60–62] measured at AGS, SPS and RHIC energies. Statistical ensembles of at least 100,0000 events are generated by CRMC EPOS 1.99 and UrQMD hybrid model at the energies 7, 7.7, 9, 11, 11.5, 13, 19, 19.6, 27, 39, 62.4, 130 and 200 GeV. In the UrQMD hybrid model, two types of the hadron-quark phase transition, namely, crossover and first order, are taken into consideration. The results from the CRMC EPOS 1.99 and the UrQMD hybrid model are compared with these measurements (symbols) and also with the HRG calculations (solid curves).

Overall, there is a convincing agreement between the HRG model calculations on the given particle ratios and the experimental results and that from the event generators, CRMC EPOS 1.99 and UrQMD. In some particle ratios, the UrQMD hybrid model seems to have a better agreement than that of the CRMC EPOS 1.99. In case of the ratio k^+/π^+,[52,53,56] we find that the HRG model agrees well with the UrQMD hybrid model and not with the CRMC EPOS 1.99 event generator. A better reproduction of the experimental data by the event generators seems not possible. There is an overestimation by HRG observed at energies $\gtrsim$10 GeV. CRMC EPOS 1.99 gives an opposite result, namely underestimation. For HRG

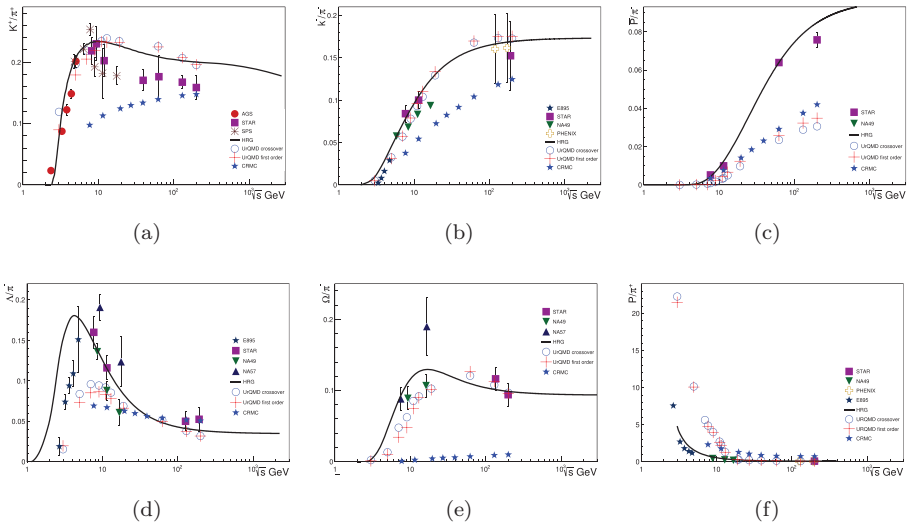

Fig. 1. Dependence of various particle ratios calculated from CRMC EPOS 1.99 (stars)[27,28] and UrQMD hybrid model[30–34] with first-order (crosses) and crossover phase-transition (empty circles) is compared with HRG calculations (solid curves)[1–8] and different experimental results (symbols) on (a) k^+/π^+,[52,53,56] (b) π^-/K^-,[52,53,56,58] (c) $\bar{p}/\pi^-$,[52,53,56,59] (d) Λ/π^-,[52–54,56,58,60,61] (e) Ω/π^-[52–54,56,58,60–62] and (f) p/π^+.[52–54,56,58,60–62]

and UrQMD hybrid model, a better situation is found in π^-/K^- and Ω/π^-, while CRMC EPOS 1.99 again underestimates both particle ratios. We also find that the HRG model describes well the STAR measurements on $\bar{p}/\pi^-$, while the corresponding event-generator results are underestimating this particle ratio. For Λ/π^-, the HRG reproduction of both experimental and simulation results is excellent, especially at energies $\gtrsim$10 GeV. The HRG model describes well p/π^+. Here both event generators overestimate p/π^+, where CRMC EPOS 1.99 is closer to HRG and experiments than UrQMD hybrid model.

Figure 2 shows the same as in Fig. 1 but here for the antiparticle-to-particle pairs like π^-/π^+ (a),[52,53,56,58] K^-/K^+ (b),[52,53,56,58] $\bar{p}/p$ (c),[52,53,56,59] $\bar{\Lambda}/\Lambda$ (d),[52–54,56,58,60,61] $\bar{\Sigma}/\Sigma$ (e)[52–54,56,58,60–62] and (f) $\bar{\Omega}/\Omega$.[52–54,56,58,60–62] Here, we also compare the experimental results with the HRG calculations and the predictions from CRMC EPOS 1.99 and UrQMD hybrid model.

We also note here that while HRG agrees excellently with the experimental results for particle ratios like $\bar{p}/p$, $\bar{\Lambda}/\Lambda$ and $\bar{\Sigma}/\Sigma$, we find that CRMC EPOS 1.99 and UrQMD hybrid model underestimate all these particle ratios. For the remaining antiparticle-to-particle ratios, we observe that the three data sets, namely, the HRG model, the collider experiments and event simulations agree well. Moreover, compared to Fig. 1, there is generally a better agreement for the experimental data of antiparticle-to-particle ratios with HRG, CRMC EPOS 1.99 and UrQMD hybrid model data. This could be understood in the light of the insubstantial fluctuations relative to the mixed particle ratios.

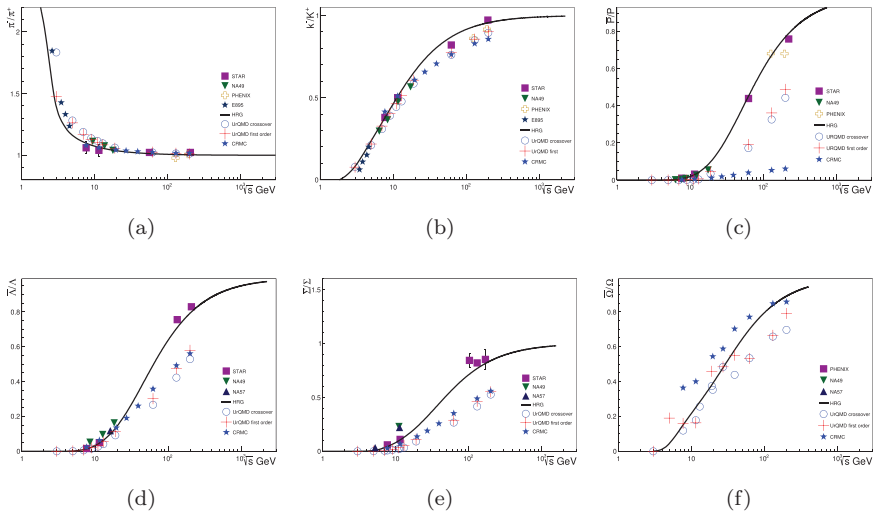

Fig. 2. The same as in Fig. 1 but here for particle-to-antiparticle ratios, (a) π^-/π^+,[52,53,56,58] (b) K^-/K^+,[52,53,56,58] (c) $\bar{p}/p$,[52,53,56,59] (d) $\bar{\Lambda}/\Lambda$,[52–54,56,58,60,61] (e) $\bar{\Sigma}/\Sigma$[52–54,56,58,60–62] and (f) $\bar{\Omega}/\Omega$.[52–54,56,58,60–62]

4. Conclusions

In this work, the CRMC EPOS 1.99 and the UrQMD hybrid model are utilized in generating statistical ensembles of 100,000 events at 7, 7.7, 9, 11, 11.5, 13, 19, 19.6, 27, 39, 62.4, 130 and 200 GeV. At these energies k^+/π^+, K^-/pi^-, $\bar{p}/\pi^-$, Λ/π^-, Ω/π^-, p/π^+, π^-/π^+, K^-/K^+, $\bar{p}/p$, $\bar{\Lambda}/\Lambda$, $\bar{\Sigma}/\Sigma$, $\bar{\Omega}/\Omega$ are determined. These results are then compared with various experiments at AGS, SPS and RHIC energies and with the HRG calculations. For the latter, the essential thermodynamic quantities, namely the temperature and the chemical potential, are determined at freezeout conditions, such as constant entropy density normalized to T^3.

For mixed particle ratios, k^+/π^+, K^-/pi^-, $\bar{p}/\pi^-$, Λ/π^-, Ω/π^-, p/π^+, π^-/π^+ there is a fair agreement between the HRG calculations and the experimental results and that from the event generators, CRMC EPOS 1.99 and UrQMD hybrid model. We conclude that the UrQMD hybrid model seems to have a better agreement than that of the CRMC EPOS 1.99. The so-called *horn* in k^+/π^+ isn't observed in both event generators, where CRMC EPOS 1.99 largely underestimates this ratio as well as the k^-/π^-. While HRG reproduces well $\bar{p}/\pi^-$, both event generators largely underestimate this particle ratio, at all energies.

For Λ/π^-, the peak at energies $\sim$10 GeV exists in all data sets. The HRG model reaches the same height as that of the experimental results, while both event generators produce smaller heights. In addition to these phenomenological observations, we find that the HRG model overestimates this ratio, at $\lesssim$7 GeV.

We also found that in almost all particle ratios the two types of the phase transitions implemented in the UrQMD hybrid model are almost indistinguishable. When

it comes to the comparison between CRMC EPOS 1.99 and UrQMD hybrid model, we find that the results deduced from the UrQMD hybrid model have generally a decent qualitative agreement with the general features of CRMC EPOS 1.99. This isn't always the case, especially for the particle ratios k^+/π^+, k^-/π^-, Ω/π^-, $\bar{p}/\pi^+$ and $\bar{\Omega}/\Omega$. Apart from the particle ratios $\bar{\Omega}/\Omega$, CRMC EPOS 1.99 seems to largely underestimate the particle ratios like k^+/π^+, k^-/π^-, Ω/π^- and $\bar{p}/\pi^+$.

Last but not least, we first conclude that the HRG model reproduces excellently the experimental results on almost all particle ratios. k^+/π^+ and Λ/π^- are the partial ratio exceptions. While HRG overestimates k^+/π^+, at $\sqrt{s_{\mathrm{NN}}} \gtrsim 10\,\mathrm{GeV}$, Λ/π^- is overestimated, at $\sqrt{s_{\mathrm{NN}}} \lesssim 10\,\mathrm{GeV}$. Second, the quality of the reproduction of the HRG model-based particle ratios by the event generators varies from particle ratio to another. Third, the same conclusion can be drawn for the quality of matching between both event generators and the experimental results.

Acknowledgment

The authors thank the anonymous referee for the important comments and suggestions to improve the paper.

References

1. P. Braun-Munzinger, J. Stachel, J. Wessels and N. Xu, *Phys. Lett. B* **365** (1996) 1.
2. A. N. Tawfik, *Int. J. Mod. Phys. A*. **29** (2014) 1430021.
3. P. Braun-Munzinger, I. Heppe and J. Stachel, *Phys. Lett. B* **465** (1999) 15.
4. J. Cleymans and H. Satz, *Z. Phys. C Part. Fields* **57** (1993) 135.
5. S. Tiwari and C. Singh, *Adv. High Energy Phys.* **2013** (2013) 805413.
6. J. Rafelski and J. Letessier, *Phys. Rev. Lett.* **85** (2000) 4695.
7. F. Becattini, J. Cleymans, A. Keränen, E. Suhonen and K. Redlich, *Phys. Rev. C* **64** (2001) 024901.
8. J. Cleymans, D. Elliott, A. Keränen and E. Suhonen, *Phys. Rev. C* **57** (1998) 3319.
9. A. N. Tawfik and I. Mishustin, *J. Phys. G*: *Nucl. Part. Phys.* **46** (2019) 125201.
10. P. Braun-Munzinger and J. Wambach, *Rev. Mod. Phys.* **81** (2009) 1031.
11. M. Gyulassy and L. McLerran, *Nucl. Phys. A* **750** (2005) 30.
12. A. Andronic, P. Braun-Munzinger, J. Stachel and M. Winn, *Phys. Lett. B* **718** (2012) 80.
13. A. Bazavov *et al.*, *Phys. Lett. B* **795** (2019) 15.
14. A. N. Tawfik, A. M. Diab and M. Hussein, *J. Phys. G*: *Nucl. Part. Phys.* **45** (2018) 055008.
15. M. A. Stephanov, *Int. J. Mod. Phys. A* **20** (2005) 4387.
16. F. Karsch, *J. Phys. G*: *Nucl. Part. Phys.* **31** (2005) S633.
17. P. Braun-Munzinger and J. Stachel, arXiv:preprint nucl-ex/9803015.
18. A. Tawfik, M. El-Bakry, D. Habashy, M. Mohamed and E. Abbas, *Int. J. Mod. Phys. E* **25** (2016) 1650018.
19. N. Kalmykov, S. Ostapchenko and A. Pavlov, *Nucl. Phys. B-Proc. Suppl.* **52** (1997) 17.
20. N. Kalmykov and S. Ostapchenko, *Phys. Atom. Nucl.* **56** (1993) 346.
21. S. Ostapchenko, *Phys. Rev. D* **74** (2006) 014026.
22. S. Ostapchenko, *Nucl. Phys. B-Proc. Suppl.* **151** (2006) 143.

23. S. Ostapchenko, Status of qgsjet, in *AIP Conf. Proc.*, American Institute of Physics, Vol. 928 (AIP, 2007), pp. 118–125.
24. J. Engel, T. Gaisser, P. Lipari and T. Stanev, *Phys. Rev. D* **46** (1992) 5013.
25. R. Fletcher, T. Gaisser, P. Lipari and T. Stanev, *Phys. Rev. D* **50** (1994) 5710.
26. E.-J. Ahn, R. Engel, T. K. Gaisser, P. Lipari and T. Stanev, *Phys. Rev. D* **80** (2009) 094003.
27. K. Werner, F.-M. Liu and T. Pierog, *Phys. Rev. C* **74** (2006) 044902.
28. T. Pierog and K. Werner, *Nucl. Phys. B-Proc. Suppl.* **196** (2009) 102.
29. H. Petersen, J. Steinheimer, G. Burau, M. Bleicher and H. Stöcker, *Phys. Rev. C* **78** (2008) 044901.
30. S. A. Bass *et al.*, *Progress Part. Nucl. Phys.* **41** (1998) 255.
31. M. Bleicher *et al.*, *J. Phys. G*: *Nucl. Part. Phys.* **25** (1999) 1859.
32. D. H. Rischke, Y. Pürsün and J. A. Maruhn, *Nucl. Phys. A* **595** (1995) 383.
33. S. Bass, M. Hofmann, C. Hartnack, H. Stöcker and W. Greiner, *Phys. Lett. B* **335** (1994) 289.
34. M. Belkacem *et al.*, *Phys. Rev. C* **58** (1998) 1727.
35. A. Tawfik, *Nucl. Phys. A* **764** (2006) 387.
36. A. Tawfik, *Europhys. Lett.* **75** (2006) 420.
37. A. Tawfik, *Nucl. Phys. A* **922** (2014) 225.
38. A. Tawfik, *Adv. High Energy Phys.* **2013** (2013) 574871.
39. A. Tawfik, *Phys. Rev. C* **88** (2013) 035203.
40. A. N. Tawfik, H. Yassin and E. R. A. Elyazeed, *Phys. Rev. D* **92** (2015) 085002.
41. D. Zschiesche, H. Stöcker, W. Greiner and S. Schramm, *Phys. Rev. C* **65** (2002) 064902.
42. M. Tanabashi *et al.*, *Phys. Rev. D* **98** (2018) 030001.
43. J. Beringer *et al.*, Particle Data Group (J. B. *et al.*), *Phys. Rev. D* **86** (2012) 010001.
44. A. Tawfik and E. Abbas, *Phys. Part. Nucl. Lett.* **12** (2015) 521.
45. L. V. Bravina *et al.*, *Phys. Rev. C* **60** (1999) 024904.
46. J. Steinheimer, S. Schramm and H. Stöcker, *Phys. Rev. C* **84** (2011) 045208.
47. J. Steinheimer *et al.*, *Phys. Rev. C* **81** (2010) 044913.
48. D. H. Rischke, Y. Pürsün and J. A. Maruhn, *Erratum-ibid. A* **596** (1996) 717.
49. T. Pierog, I. Karpenko, J. M. Katzy, E. Yatsenko and K. Werner, *Phys. Rev. C* **92** (2015) 034906.
50. A. Bzdak *et al.*, *Phys. Rep.* **853** (2020) 1.
51. T. Anticic *et al.*, *Phys. Rev. Lett.* **93** (2004) 022302.
52. S. Afanasiev *et al.*, *Phys. Lett. B* **358** (2002) 275.
53. C. Alt *et al.*, *Phys. Rev. Lett.* **94** (2005) 192301.
54. S. Afanasiev *et al.*, *Phys. Rev. C* **66** (2002) 054902.
55. C. Blume *et al.*, *J. Phys. G*: *Nucl. Part. Phys.* **31** (2005) S685.
56. F. Antinori *et al.*, *Phys. Lett. B* **595** (2004) 68.
57. A. N. Tawfik *et al.*, *Eur. Phys. J. A* **52** (2016) 1.
58. J. Klay *et al.*, *Phys. Rev. Lett.* **88** (2002) 102301.
59. J. Klay *et al.*, *Phys. Rev. C* **68** (2003) 054905.
60. P. Chung *et al.*, *Phys. Rev. Lett.* **91** (2003) 202301.
61. C. Pinkenburg, arXiv:preprint nucl-ex/0104025.
62. B. Back *et al.*, *Phys. Rev. C* **69** (2004) 054901.